

# **$^{99m}\text{Tc}$ MDP SPECT/CT imaging in the evaluation of mandibular osteomyelitis severity**

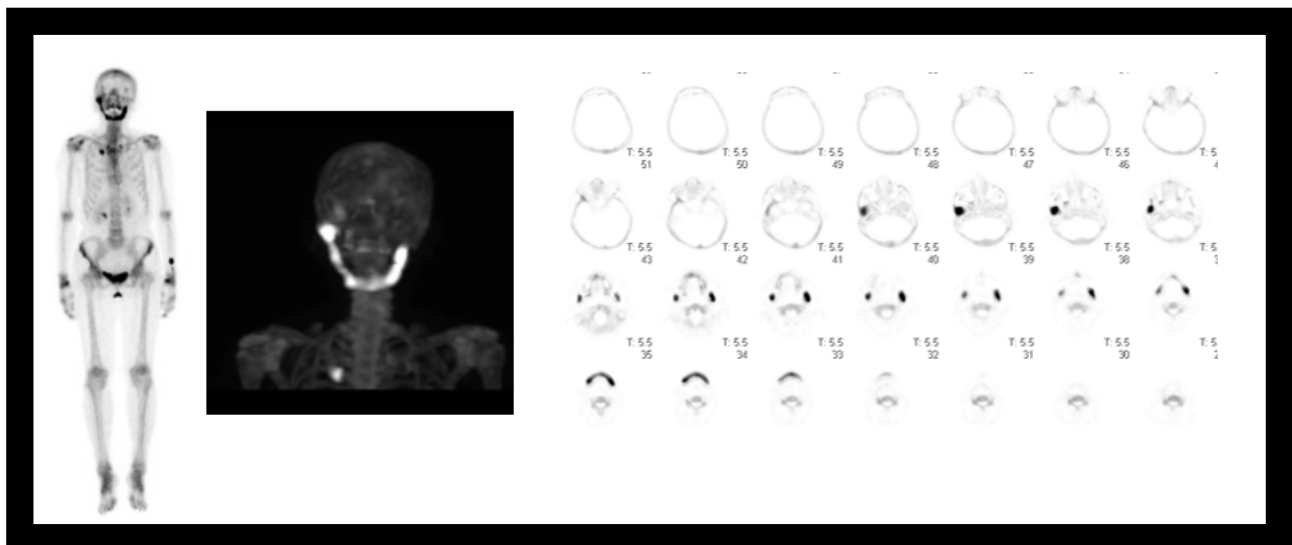
By Partha Ghosh, MD, Siemens Healthineers, Hoffman Estates, IL, USA  
Data and images courtesy of Chiba Aoba Municipal Hospital, Chiba, Japan

## **History**

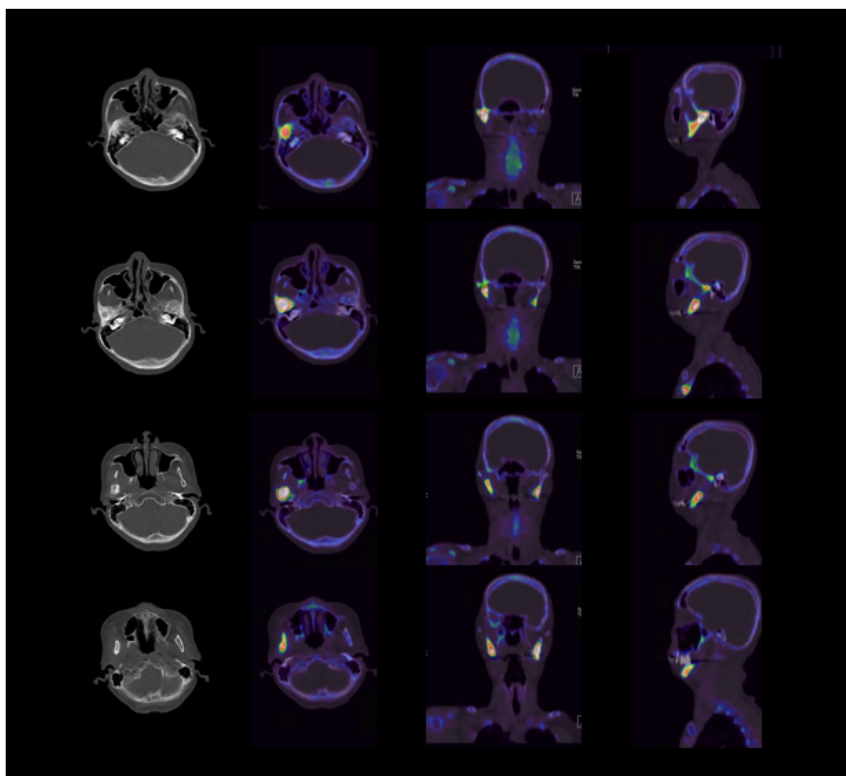
A 67-year-old female reported chronic pain and limited movement in her right temporo-mandibular joint along with difficulty opening her jaw.

Clinical examination showed ankylosis of the right-mandibular joint with extremely restricted movement, suggesting that surgical replacement of the affected mandible with a prosthesis may be difficult.

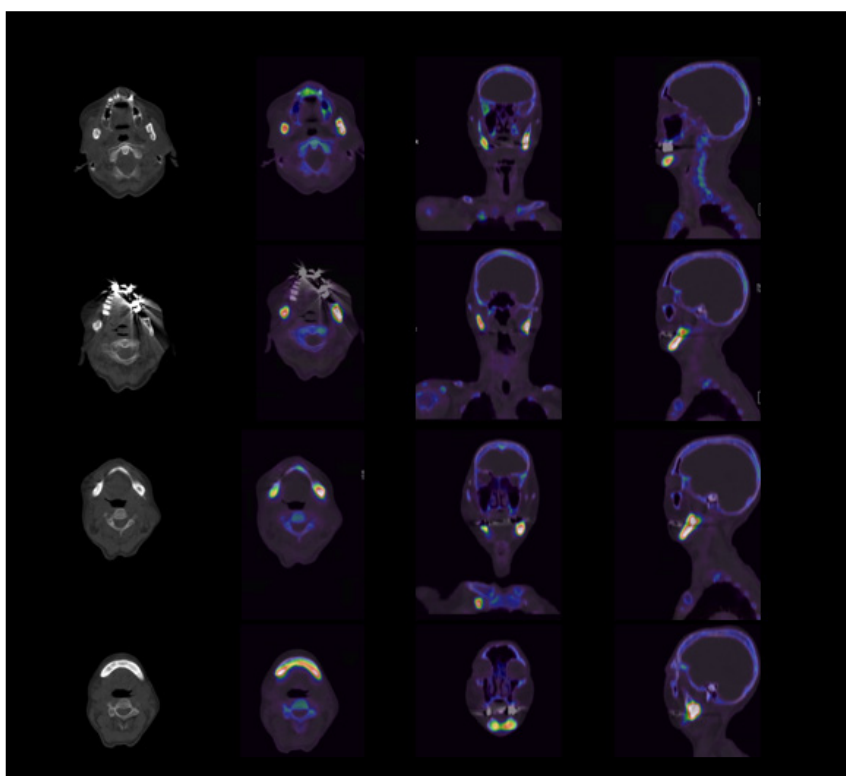
A  $^{99m}\text{Tc}$  MDP bone scintigraphy with whole-body planar and SPECT/CT of the head-and-neck region was performed to delineate the extent of mandibular pathology.



**1** Whole-body planar, SPECT MIP, and axial sections of the  $^{99m}\text{Tc}$  MDP bone study show intense hypermetabolism in the mandible, especially in the right mandibular condylar process. The right mandibular ramus and body also show a moderate increase in uptake, while the body and part of the ramus on the left side of the mandible reflect intense uptake. The left condylar process is free of any hypermetabolism. MIP and axial slices of the SPECT study indicate relative similarity in uptake intensity in the right mandibular condylar process and the left ramus.

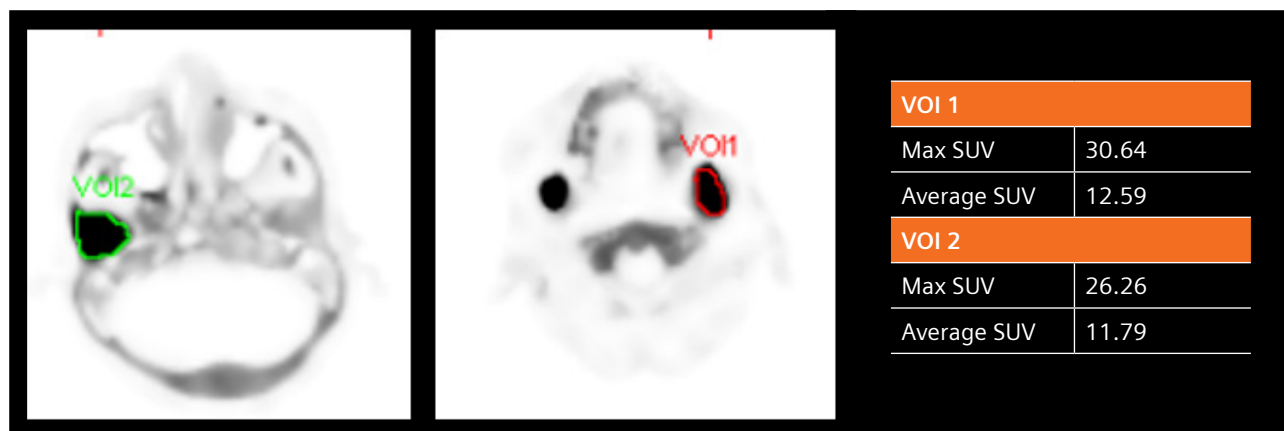


**2** Axial CT and fused SPECT/CT images in different orientations show intense sclerosis involving the right mandibular condylar process with corresponding intense hypermetabolism in the condyle as well as the adjacent ramus correlating with ankylosis of the right temporo-mandibular joint. The fused images also show intense hypermetabolism in the right as well as the left mandibular ramus.

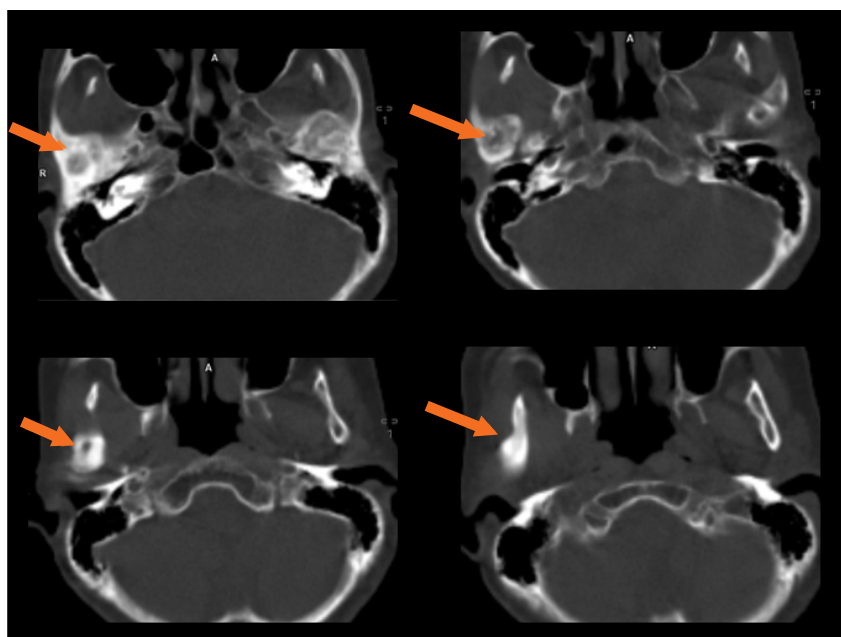


**3** Axial CT slices and fused SPECT/CT slices in various orientations show sclerosis within the ramus and the body of the right and left sides of the mandible with corresponding hypermetabolism, suggesting involvement of the entire mandible except for the left condylar process.

As indicated in Figures 1-3, the initial SPECT/CT study showed severe sclerosis and hypermetabolism in the right mandibular condylar process with ankylosis of the right mandibular joint along with involvement of the entire ramus and body of the right and the left mandible. Both the sclerosis and hypermetabolism were particularly high and of similar intensity in the right condylar process and left ramus, suggesting two foci of particular intensity in these areas with a lower level of involvement in the rest of the mandibular body. The sparing of the left mandibular condylar process and the left temporo-mandibular joint of any pathology is clearly defined in the MIP and the fused images.



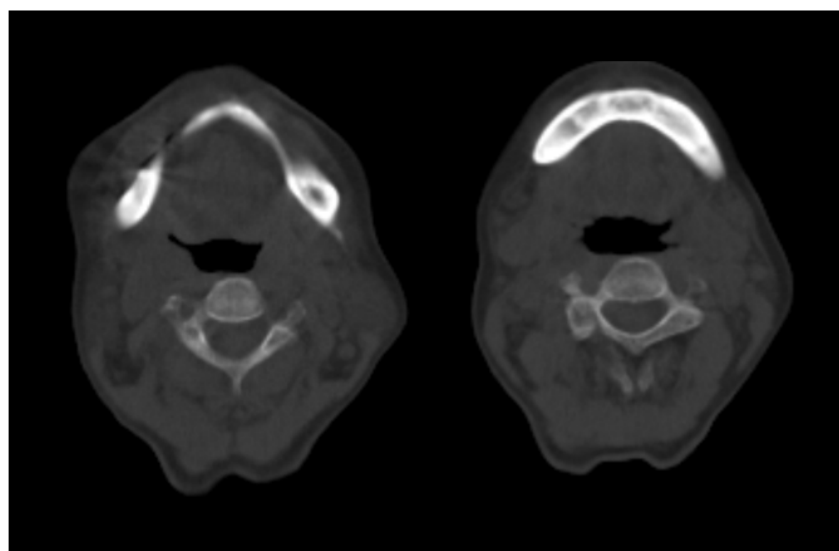
- 4 SUV estimation from xSPECT Quant denotes an  $SUV_{max}$  of 30.6 in the right mandibular condyle (Vol 2-Green) and an  $SUV_{max}$  of 26.2 in the left ramus (Vol 1-Red). The quantitative SPECT/CT enables the evaluation of  $SUV_{max}$  and  $SUV_{peak}$  to establish a quantitative benchmark for subsequent follow-up.



- 5 The zoomed image of the CT axial slices through the mandibular condylar process and the upper part of the mandibular ramus shows osteosclerosis, periosteal, and cortical bone thickening as well as perforations or breakage of the cortical bone at some points in the right and the left mandibular ramus. These features suggest the possibility of osteonecrosis or osteomyelitis of the mandible.

## Findings

The SPECT/CT findings show typical CT changes of osteosclerosis, periosteal, and cortical bone thickening, as well as an intense and variegated hypermetabolism in the mandible with particularly intense foci in the right mandibular condylar process; in addition, the ankylosis of the right mandibular joint along with an intense hypermetabolism and sclerosis in the left mandibular ramus, suggest the possibility of severe and diffuse mandibular osteomyelitis. This may be due to a gingival infective foci or osteomyelitis secondary to a mandibular osteonecrosis, which could be related to diphosphonate use. In review of the age and gender of the patient (67-year-old female), the possibility of mandibular osteonecrosis secondary to diphosphonate use is deemed a distinct possibility and needs to be ruled out by conducting a thorough assessment of her medication history. The patient was treated conservatively with antibiotics but continued to display symptoms of pain and extremely restricted jaw movement. A  $^{67}\text{Ga}$  scintigraphy conducted two years prior showed limited active

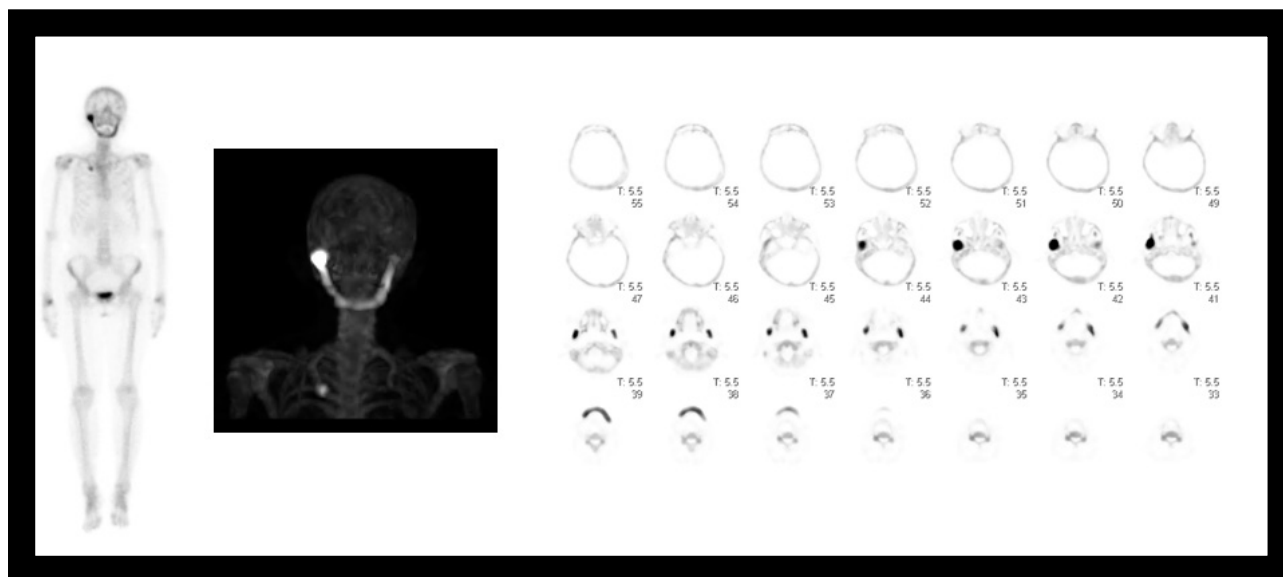


**6** The lower part of the ramus and the body of the mandible visualize osteosclerosis and cortical bone thickening, reflecting osteonecrosis or osteomyelitis.

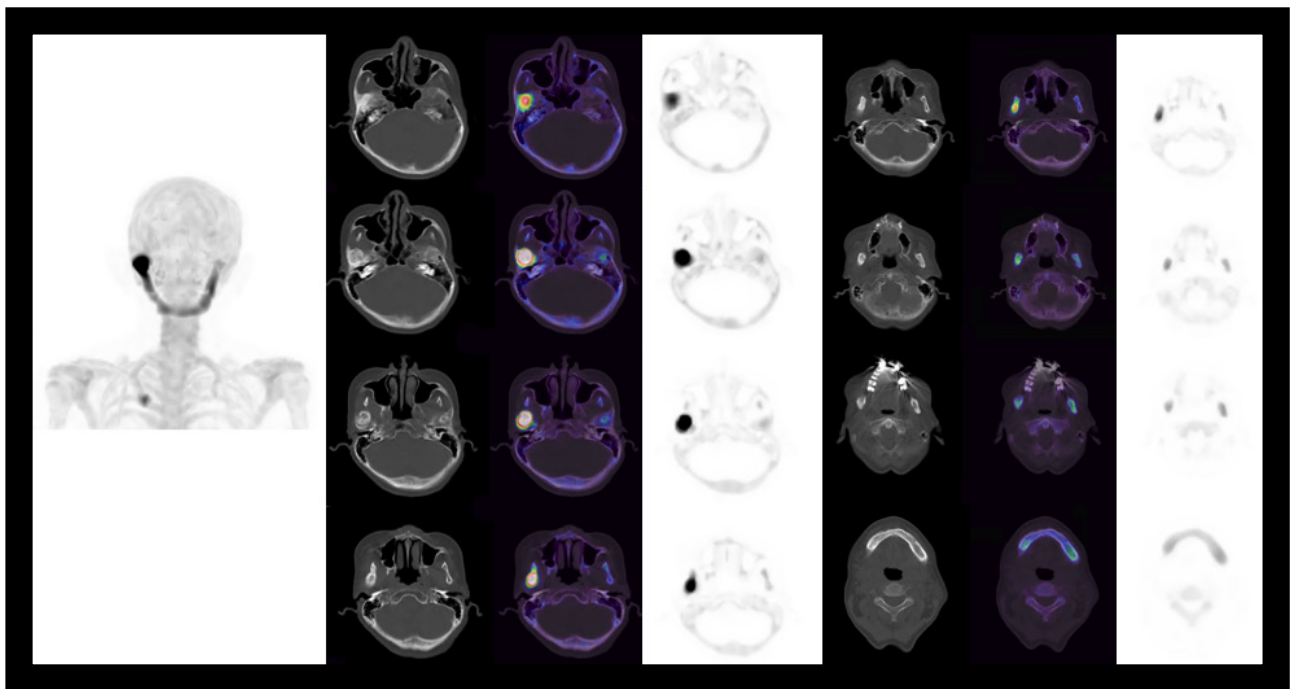
osteomyelitis (right mandibular joint; left mandibular superior branch), ruling out multiple myeloma.

Two years following the initial  $^{67}\text{Ga}$  scintigraphy, the patient underwent a  $^{99\text{m}}\text{Tc}$  MDP SPECT/CT study on a Symbia Intevo™ scanner equipped with xSPECT Bone™ and xSPECT Quant™ to assess the morphological and metabolic change to the mandib-

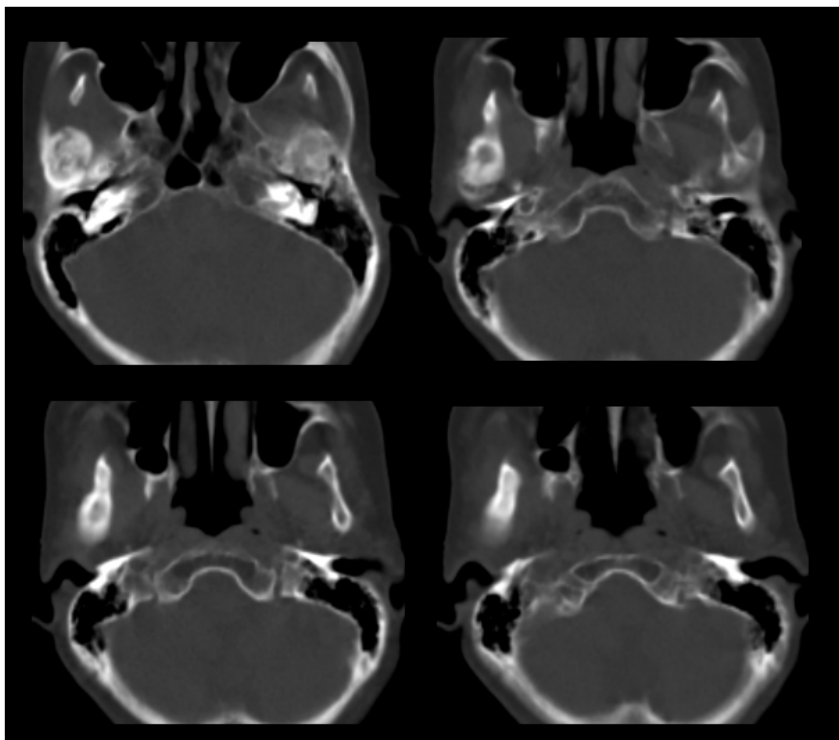
ular osteomyelitic process. The study was performed 3 hours following an intravenous IV injection of 23.7 mCi (878.7 MBq). A whole-body planar study was performed followed by a SPECT/CT. Additionally, xSPECT Bone and xSPECT Quant reconstructions were performed and fused with CT for evaluation.



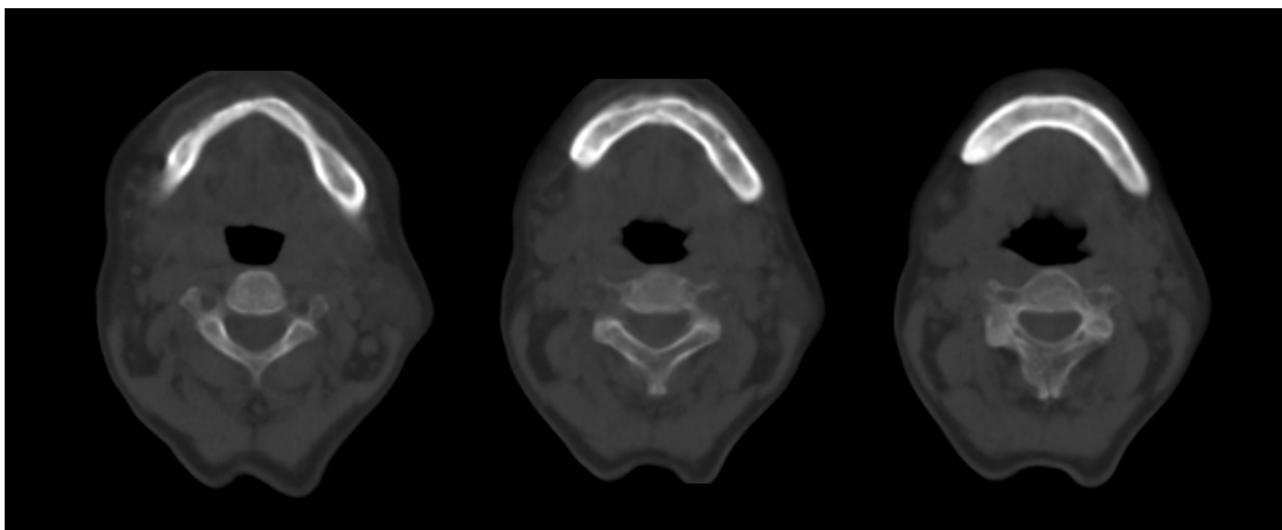
**7** Whole-body planar, MIP, and axial slices of the SPECT study reveal intense uptake in the right mandibular condylar process with lower intensity of uptake in the right and left ramus in addition to the body. The left mandibular condyle is free of any hypermetabolism.



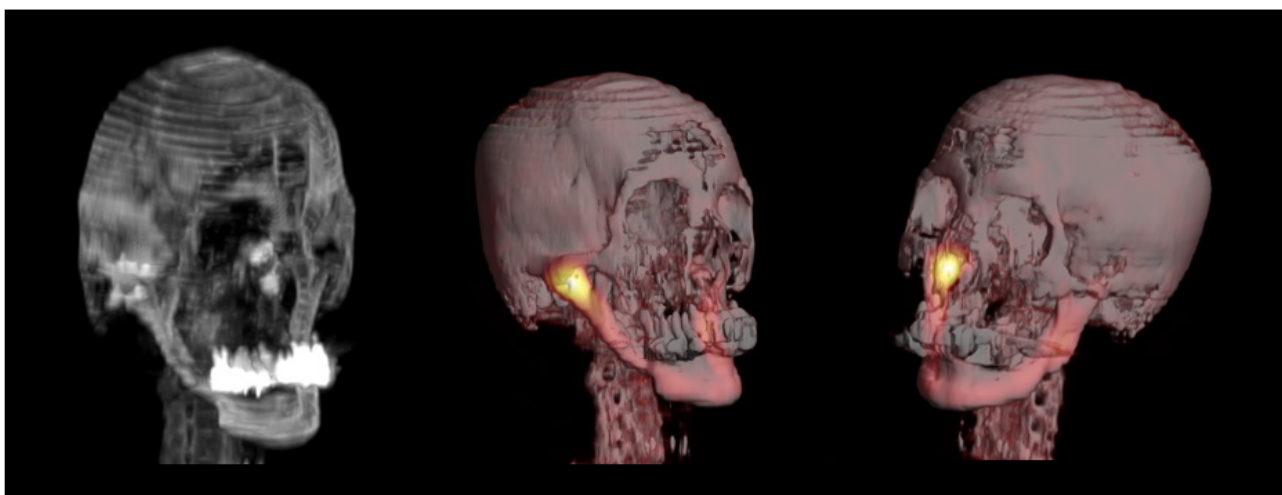
**8** MIP, xSPECT Bone, CT, and fused SPECT/CT axial slices show intense uptake in the right mandibular condylar process comparable to the initial study but with slightly lower uptake intensity in the rest of the mandible, especially in the left ramus. The level of osteosclerosis remains similar to that of the initial study.



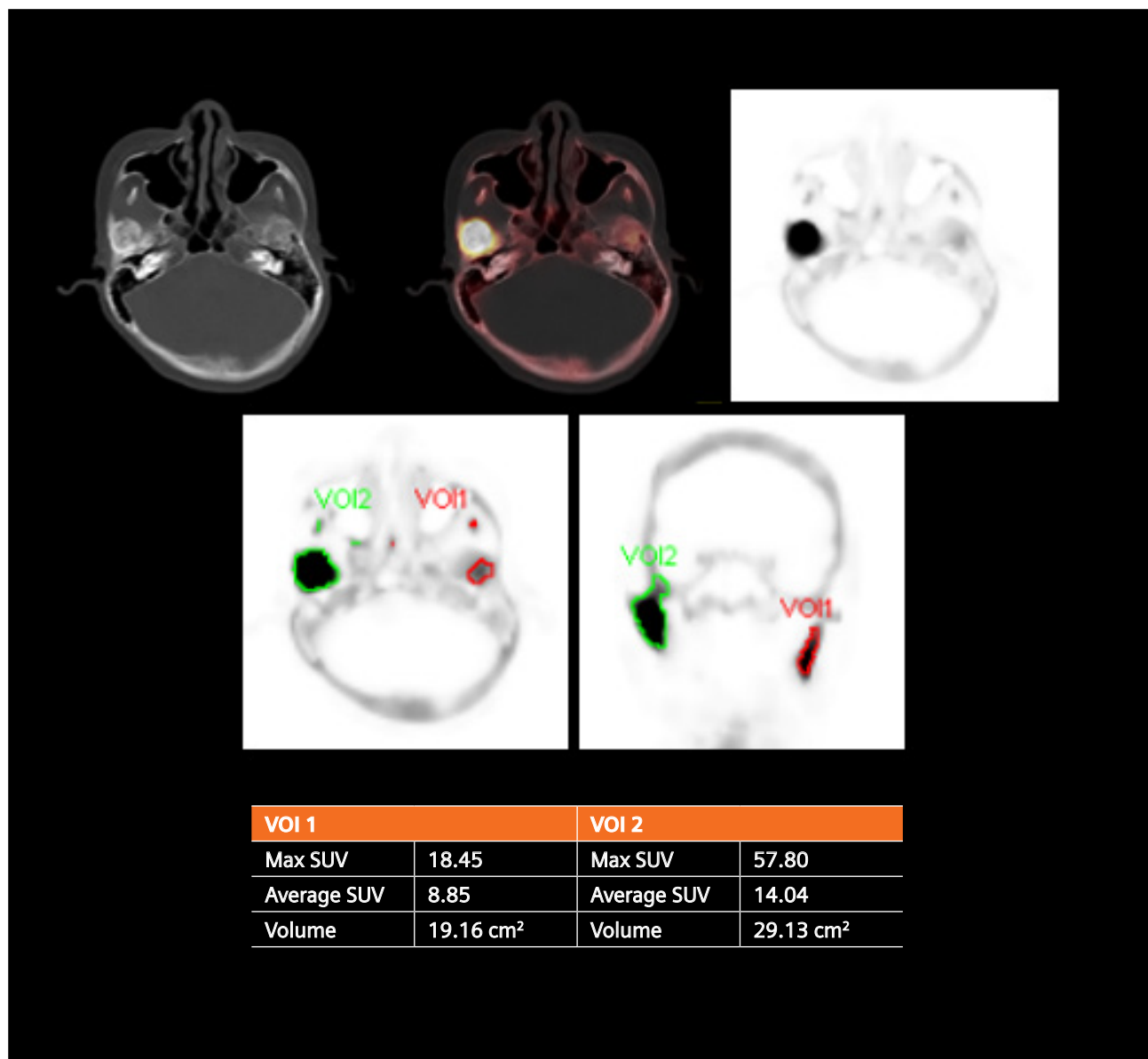
**9** The zoomed CT images from the follow-up study also show osteosclerosis with small focal areas of osteolysis along with cortical and periosteal thickening and cortical perforation in the right mandibular condylar process, as well as the adjacent right and left mandibular ramus. The sclerosis intensity is similar to that of the initial study.



**10** Axial slices through the body of the mandible show focal sclerosis, cortical bone thickening, periosteal thickening, and cortical perforations typical of mandibular osteomyelitis.



**11** CT MIP as well as volume rendering of fused SPECT/CT reveal sclerosis with corresponding intense hypermetabolism in the right mandibular condylar process and the right temporo-mandibular joint. The ramus and body of the mandible highlight cortical sclerosis but with lesser extent of hypermetabolism. The dental implants in the upper jaw cause beam-hardening artifacts in the CT, impacting the visualization of parts of the mandibular ramus.



**12** xSPECT Quant-based SPECT/CT quantification shows  $SUV_{max}$  in the right mandibular condylar process (Vol 2-Green) to be 57.8 and the left mandibular ramus (Vol 1-Red) to be 18.4.

Although the visual impression of the sequential SPECT suggests a resolution of the intensity of uptake in the left ramus—including the continuation of similar hypermetabolism levels in the right mandibular condylar process—the xSPECT Quant quantitative evaluation confirms the significant increase in hypermetabolism in the right mandibular condyle

in addition to and the decrease in left ramus uptake. Likewise, the follow-up SPECT suggests a resolution of the intensity of uptake in the left ramus—including the continuation of similar hypermetabolism levels in the right mandibular condylar process. However, the xSPECT Quant quantitative evaluation confirms the significant increase in hypermetabolism in the

right mandibular condyle. The decrease in the left ramus reflects a variegated response to antibiotic therapy with complicating processes of ankylosis in the right mandibular joint, which may further increase the osteosclerotic and osteolytic processes, leading to higher metabolism.

## Initial study



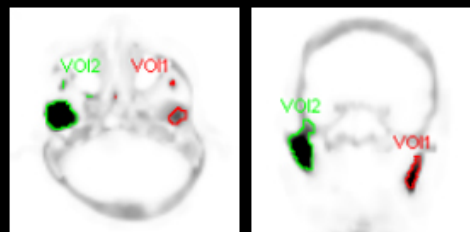
## VOI 1

Max SUV	30.64
Average SUV	12.59

## VOI 2

Max SUV	26.26
Average SUV	11.79

## Follow-up study

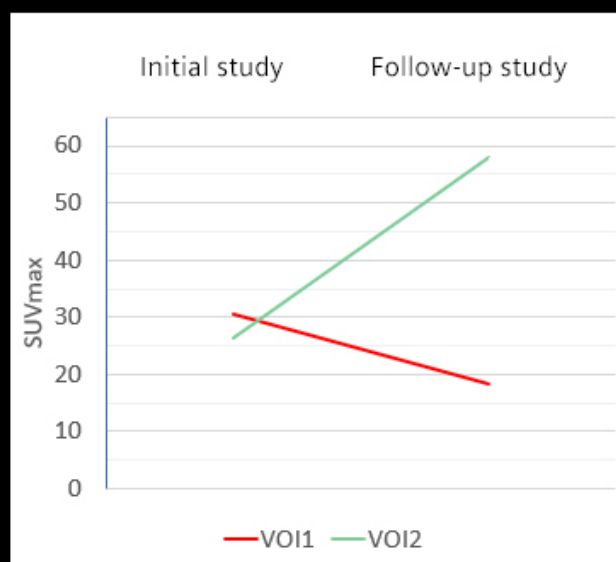


## VOI 1

Max SUV	18.45
Average SUV	8.85
Volume	19.16 cm <sup>2</sup>

## VOI 2

Max SUV	57.80
Average SUV	14.04
Volume	29.13 cm <sup>2</sup>



- 13 The comparison of  $SUV_{max}$  between the initial and follow-up xSPECT Quant studies shows a significant increase in  $SUV_{max}$  in the right mandibular condylar process pathology. This significant increase from 26.2 to 57.8 suggests advanced severity of the mandibular osteomyelitis with a higher hypermetabolism reflecting advanced ankylosis and sclerosis. However, the hypermetabolic area of the osteomyelitis in the left mandibular ramus shows a decrease in  $SUV_{max}$  from 30.5 to 18.4—which is also reflected in the visual intensity of uptake in the left mandibular ramus—suggesting a partial resolution of the osteomyelitic process in that segment of the mandible. The  $SUV_{max}$  trend chart also reflects the differential response of  $SUV_{max}$  in two different mandibular zones.

## Discussion

Mandibular osteomyelitis may be caused by bacterial infections of the teeth and gums and may occur secondary to medication-related osteonecrosis of the mandible and maxillofacial region.<sup>1</sup> Medication-related osteonecrosis of the jaw is often related to bisphosphonate therapy for osteoporosis in the elderly.

In this patient, the severity of osteomyelitis was advanced in the right mandibular condylar process with gross sclerosis and fibrosis with ankylosis of the right temporo-mandibular joint. However, the osteomyelitis process also spread to the right mandibular ramus and body and also to the left body and ramus, thereby involving nearly the entire mandible and sparing only the left mandibular condyle and left temporo-mandibular joint.

The CT changes of sclerosis, focal osteolysis, cortical and periosteal thickening, and cortical perforations are typical of mandibular osteomyelitis, although it is not possible to differentiate between bacterial infection-related mandibular osteomyelitis and osteomyelitis secondary

to medication-related osteonecrosis of the jaw.<sup>2</sup> Furthermore, the CT changes are not reflective of a response of the osteomyelitic process following antibiotic therapy, since the established sclerosis is not altered with therapy.

In this context, quantitative SPECT/CT may be helpful in assessing response and progression of disease process, as evident from the SUV evaluation using sequential xSPECT Quant, which clearly shows resolution in the left ramus with progression in the right mandibular condylar process. Ogura et al performed a quantitative SPECT/CT in 9 patients with medication-related jaw osteonecrosis and 4 patients with chronic mandibular osteomyelitis. The  $SUV_{max}$  was consistently higher in chronic osteomyelitis (mean  $SUV_{max}$  10.16) compared to that in medication-related osteonecrosis (mean  $SUV_{max}$  5.50).<sup>3</sup> The estimation of total bone uptake—attained by multiplying the  $SUV_{mean}$  with the metabolic bone volume measured by the volume of interest (VOI) around the lesion—was also significantly higher in chronic osteomyelitis.

Although the current study is focused on  $SUV_{max}$  within lesions, the estimations of metabolic bone volume from the VOI may be easily obtained for calculation of total bone uptake from the xSPECT Quant data using syngo®.via software. This could further improve evaluation of extensive disease processes, which in this case, involves nearly the entire mandible. The severity of  $SUV_{max}$  increase in the right mandibular joint may have multi-factorial causes, including progression of the chronic osteomyelitic process and progressive ankylosis, limitation of movement, and further alteration of bone metabolism. The left ramus lesion appears to have responded to therapy, as reflected in the decrease in  $SUV_{max}$ .

## Conclusion

xSPECT Quant helps provide a reproducible and automated quantitative solution for the sequential evaluation of complicated disease processes. In combination with CT changes evaluated using diagnostic CT as part of the SPECT/CT process, this offers a comprehensive assessment of mandibular osteomyelitis. ●

## Examination protocol

Scanner: Symbia Intevo 6

SPECT		CT	
Injected dose	23.7 mCi (878.7 MBq) <sup>99m</sup> Tc MDP	Tube voltage	130 kV
Post-injection delay	3 hours	Tube current	13 eff mAs
Acquisition	30 stops/detector, 20 seconds/stop	Slice collimation	6 x 2 mm
		Slice thickness	5 mm
		Reconstruction kernel	B70s

The outcomes achieved by the Siemens Healthineers customers described herein were achieved in the customer's unique setting. Since there is no "typical" hospital and many variables exist (e.g. hospital size, case mix, level of IT adoption) there can be no guarantee that others will achieve the same results.

## References

- <sup>1</sup> Kato H, Uchibori M, Nakanishi Y, Kaneko A. A Case of Osteomyelitis of the Mandibular Condyle Secondary to Bisphosphonate-related Osteonecrosis of the Jaw. *Tokai J Exp Clin Med.* 2020;45(3):126-130. PMID:32901900.
- <sup>2</sup> Malina-Altzinger J, Klaeser B, Suter VGA, Schriber M, Vollnberg B, Schaller B. Comparative evaluation of SPECT/CT and CBCT in patients with mandibular osteomyelitis and osteonecrosis. *Clin Oral Investig.* 2019;23(12):4213-422. doi:10.1007/s00784-019-02862-8.
- <sup>3</sup> Ogura I, Kobayashi E, Nakahara K, Igarashi K, Haga-Tsujimura M, Toshima H. Quantitative SPECT/CT imaging for medication-related osteonecrosis of the jaw: a preliminary study using volume-based parameters, comparison with chronic osteomyelitis. *Ann Nucl Med.* 2019;33(10):776-782. doi:10.1007/s12149-019-01390-5.

**Legal information:** On account of certain regional limitations of sales rights and service availability, we cannot guarantee that all products included in this publication are available through the Siemens Healthineers sales organization worldwide. Availability and packaging may vary by country and is subject to change without prior notice.

The information in this document contains general technical descriptions of specifications and options as well as standard and optional features, which do not always have to be present in individual cases.

Please contact your local Siemens Healthineers sales representative for the most current information.

Note: Any technical data contained in this document may vary within defined tolerances. Original images always lose a certain amount of detail when reproduced.

“Siemens Healthineers” is considered a brand name. Its use is not intended to represent the legal entity to which this product is registered. Please contact your local Siemens Healthineers organization for further details.

---

**Siemens Healthineers Headquarters**

Siemens Healthcare GmbH  
Henkestr. 127  
91052 Erlangen  
Germany  
Phone: +49 9131 84-0  
[siemens-healthineers.com](https://www.siemens-healthineers.com)

**Published by**

Siemens Medical Solutions USA, Inc.  
2501 N. Barrington Road  
Hoffman Estates, IL 60192-2061  
USA  
Phone: +1 847-304-7700  
[siemens-healthineers.com/mi](https://www.siemens-healthineers.com/mi)